Interactive CardioVascular and Thoracic Surgery 16 (2013) 743–749
doi:10.1093/icvts/ivt036 Advance Access publication 6 March 2013

Four-dimensional geometric assessment of tricuspid annulus movement in early functional tricuspid regurgitation patients indicates decreased longitudinal flexibility

Satoru Maeba[a,*], Takahiro Taguchi[a], Hirofumi Midorikawa[b], Megumu Kanno[b] and Taijiro Sueda[c]

[a] Department of Cardiovascular Surgery, Takeda General Hospital Foundation, Fukushima, Japan
[b] Department of Cardiovascular Surgery, Southern Tohoku General Hospital, Fukushima, Japan
[c] Department of Cardiovascular Surgery, Hiroshima University Hospital, Hiroshima, Japan

*Corresponding author: Department of Cardiovascular Surgery, Takeda General Hospital Foundation, 3-27 Yamaga-machi, Aizuwakamatsu, Fukushima 965-8585, Japan. Tel: +81-242-299932; fax: +81-242-292726; e-mail: cardiosatoru@hotmail.com (S. Maeba).

Received 4 July 2012; received in revised form 2 January 2013; accepted 9 January 2013

Abstract

OBJECTIVES: Functional tricuspid regurgitation (FTR) is generally caused by the dilation of the tricuspid annulus (TA) and the tethering of tricuspid leaflets; however, it also occurs in patients without dilatation of the TA. The aim of this study was to develop and to use a four-dimensional tracking system, utilizing cardiac magnetic resonance imaging (MRI), and to assess TA flexibility in patients with early FTR without right ventricle dilation as a preliminary investigation for the mechanism of early FTR.

METHODS: The structure and movement of the TA were examined in 20 healthy subjects and 19 FTR patients whose right ventricle was not dilated. We analysed the short axis and longitudinal movement of a mid-septal point (S), a mid-lateral point (L), a mid-anterior point (A) and a mid-posterior point (P) on the TA throughout the cardiac cycle. The tethering distance of the tricuspid leaflets and the integrated orbiting volume of the TA were also measured.

RESULTS: The TA area (mm^2) and AP and LS distances (mm) did not differ significantly between the two groups, but the longitudinally moving distances (mm) of the four points were significantly shorter in patients with FTR than in healthy subjects. Also, the mean tethering distance (mm) was significantly longer in patients with FTR than in healthy subjects (9.0 ± 1.5 vs 4.0 ± 1.3, respectively; $P < 0.001$), and the integrated volume (mm^3) of the annular moving track, throughout the cardiac cycle, was significantly larger in healthy subjects than in patients with FTR (40 428 ± 10 951 vs 22 967 ± 6079, $P < 0.001$).

CONCLUSIONS: The longitudinal flexibility of the TA in FTR patients was significantly less than that in the healthy subjects, and the tethering of the tricuspid leaflets occurred in FTR patients despite the absence of TA and RV dilation, which can be one triggering factor of early FTR. Four-dimensional geometric assessment, using cardiac MRI and the tracking program that we have developed, is capable of determining TA structure and flexibility.

Keywords: Tricuspid regurgitation • Tricuspid annulus • Longitudinal flexibility • Cardiac MRI • Cardiac valve annulus

INTRODUCTION

Tricuspid regurgitation can result from alterations in any one or all the components [e.g. the leaflets, chordae tendineae, annulus and papillary or adjacent right ventricular (RV) muscles] of the tricuspid valve (TV) apparatus. It is classified as primary when caused by an intrinsic abnormality and secondary when caused by RV dilatation. Secondary residual functional tricuspid regurgitation (FTR) is common following left-sided heart valve surgery. Here, the main mechanism of FTR is thought to be the secondary effect following the annular dilation and the tethering of leaflets associated with RV dilation [1–3].

Tricuspid regurgitation resulting from myocardial dysfunction or dilatation is associated with poor prognosis, including a mortality of up to 50% in 5 years [4–6]. With surgical intervention, prognosis is improved. Tricuspid annuloplasty using prosthetic bands is the preferred intervention for FTR. However, even after tricuspid annuloplasty, residual FTR can persist [7, 8]. This discrepancy may result from a disconnect between the goal of tricuspid annuloplasty and the mechanism responsible for FTR in these patients.

Recently, geometric assessments of the tricuspid annulus (TA) by real-time three-dimensional (3D) echocardiography have determined that the structure of the TA in FTR patients is more planar than in healthy subjects [9, 10]. The authors concluded that the flattening of the annulus may cause the lowest point of the annulus to be stretched away from the papillary muscles, increasing the tethering of leaflets. In order to reconstruct the annulus and correct this flattening, some surgeons prefer a 3D rigid band. Although this procedure has resulted in good

mid-term outcomes, 10–14% of patients receiving a 3D rigid band still suffered from significant tricuspid regurgitation progression after the operation [11, 12]. In addition, we frequently encounter cases of FTR that are not associated with RV dilation, particularly when patients have chronic atrial fibrillation and a dilated atrium. These observations indicate that other mechanisms may be responsible for early FTR, and therefore, alternative procedures for tricuspid repair may be required. The reappraisal of techniques to eliminate FTR should be based on a more accurate geometric assessment of the TA.

Cardiac imaging techniques, including echocardiography, are extremely useful in identifying whether FTR is the result of structural abnormalities or myocardial dysfunction and dilatation. Doppler techniques are useful for the visualization of regurgitant jets, the measurement of flow velocities and the estimation of RV systolic pressure. However, when it comes to accurate geometric assessment of the heart, cardiac magnetic resonance imaging (MRI) offers advantages over echocardiography. Geometric assessment by real-time 3D echocardiography can provide clear images of structure; however, deriving accurate and reliable quantitative data from these images is difficult as echovectors vary depending on the location of the ribs and lungs. Cardiac MRI offers superior tissue contrast and high spatial and temporal resolution and enables the accurate tracing of specific points.

The objective of this study was to develop and use a 4D tracking system utilizing cardiac MRI and to assess TA flexibility in patients with early FTR, without TA and RV dilation, as a preliminary investigation for the mechanism of early FTR.

METHODS

Study participants

The study population consisted of 20 healthy volunteers (10 males and 10 females; mean age 32.2 ± 9.4 years) and 19 patients (11 males and 8 females; mean age 76.8 ± 7.0 years) with moderate or severe FTR and non-dilated RV who had received cardiac MRI. Healthy volunteers had no history and no evidence of heart disease. The degree of tricuspid regurgitation was assessed by 2D transthoracic echocardiography, and the maximal jet area in any view was used to estimate the regurgitation grade, using the standard colour Doppler technique. Severe tricuspid regurgitation was defined as a tricuspid regurgitation jet area of >10 cm^2. Non-dilated RV was defined as the RV volume index of <100 ml/m^2 [13]. RV function was assessed by fractional change in the RV area, in the apical four-chamber view.

Of the 19 patients, 18 were candidates for left-sided heart surgery, and the primary underlying left-sided diseases were mitral regurgitation and/or stenosis (12 patients), aortic stenosis (5 patients) and ischaemic cardiomyopathy (1 patient). The final patient had FTR complicated with severe emphysema. This study was approved by the Ethics Committee of the Takeda General Hospital Foundation.

Cardiac magnetic resonance imaging

MRI studies were performed with a 1.5-T MRI (Phillips Medical Systems, Best, Netherlands) equipped with a 32-element Torsor cardiac coil. A cardiac-triggered, steady-state, free-precession sequence was used for quantitative analysis. Images were acquired during breath-holding using prospective electrocardiogram gating, and most cases required two breath-hold phases to complete all imaging. The temporal resolution was 30–50 ms/frame, and 20 frames per heart beat were acquired for each slice.

The additional imaging parameters for the cine acquisition were: repetition time (RT) = shortest, echo time (TE) = shortest, flip angle = 55 degree, scan matrix = 192 × 122 (reconstructed to 256 × 256 pixels), field of view = 35 × 35 cm and slice thickness = 8 mm/gap = 1 mm (four-chamber vertical slice thickness = 10 mm/gap = 2 mm). Initial scouting images were also taken and reference scans were performed.

We located four points (mid-septal, mid-lateral, mid-anterior and mid-posterior) on the TA (Fig. 1) using the following procedures. First, we used four-chamber cine imaging to measure the RV end-systolic and end-diastolic areas (RV-EsA and RV-EdA) and to identify mid-septal (S) and mid-lateral (L) points. Once the rotational axis was defined, as the vector orthogonal to the TA plane (approximately parallel to the ventricular septal wall) and passing through the centre of the TA, the scanning plane was rotated at 90° to scan the vertical long-axis cine (pseudo two-chamber view), trace a mid-anterior point (A) and

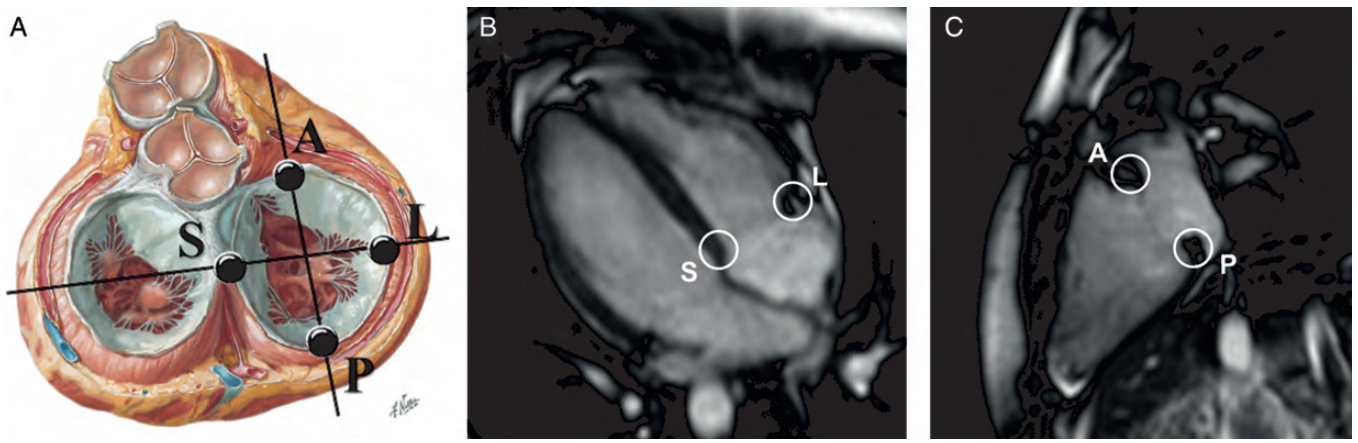

Figure 1: Tracing of the four points on the tricuspid annulus. (**A**) Schematic diagram indicating the position of the four points [mid-septal (S), mid-lateral (L), mid-anterior (A) and mid-posterior (P)]; (**B**) image showing the location and example of tracing for S and L points; (**C**) image showing the location and example of tracing for A and P points.

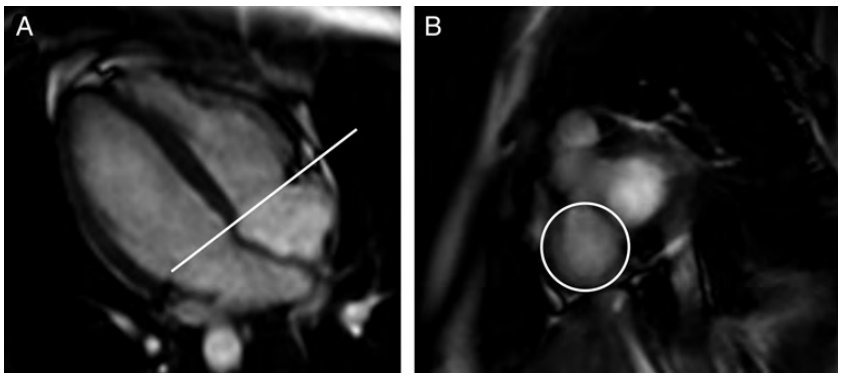

Figure 2: Determination of horizontal short-axis planes used to determine the tricuspid annular area. (**A**) Image showing the four-chamber view and the tricuspid annular line to obtain the short-axis plane of the tricuspid annulus (TA). (**B**) Image showing the short-axis plan of the TA.

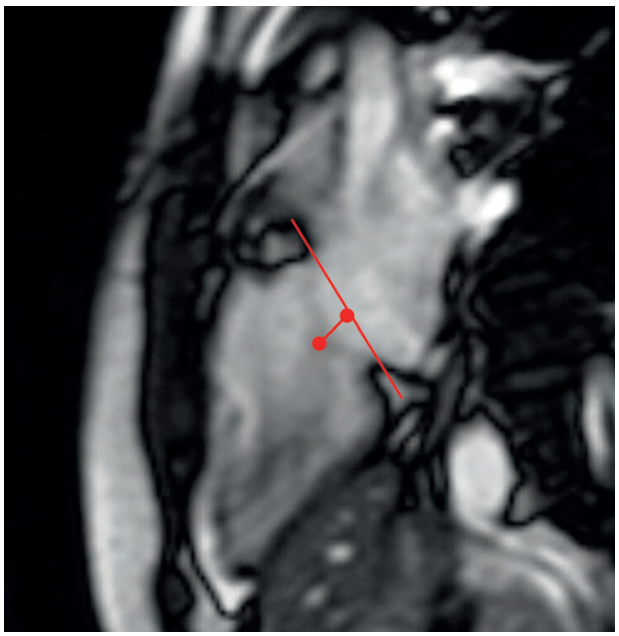

Figure 3: The measurement of the tricuspid leaflet tethering height. Tethering height was determined by measuring the distance between the annular plane and the coapted point (distance between two red points).

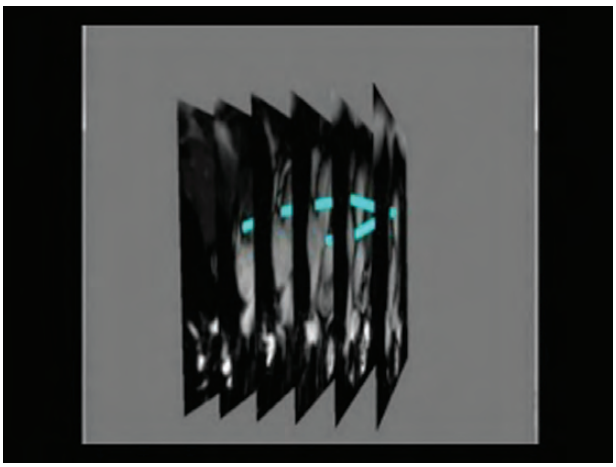

Supplementary Video S1: Animation showing the 4D movement of a tricuspid annulus (TA) outline, created using a 3D spline-curving procedure. This technique enables the assessment of TA flexibility and allows determining the orbit volume of the annulus.

determine a mid-posterior point (P). By bisecting this rotational axis, horizontal short-axis planes of the annulus (Fig. 2) and RV were determined. These were used to measure the tricuspid annular area (TAA) and RV volume. RV area and volume were normalized to the body surface area.

The above procedures produced the following types of data:

(i) The RV-EsA and RV-EdA indices (mm^2/m^2) in an apical four-chamber view and the RV end-diastolic volume index (RV-EdV index; ml^2/m^2). RV volume was calculated by summing the volume of each slice with Simpson's rule.
(ii) RV ejection fraction (RVEF; %); RVEF was calculated as (RV-EdA – RV-EsA)/RV-EdA × 100 [14].
(iii) AP distance (mm), during mid- and end-systole and mid- and end-diastole phases of the cardiac cycle.
(iv) LS distance (mm), during mid- and end-systole and mid- and end-diastole phases of the cardiac cycle.
(v) TAA (mm^2), during mid- and end-systole and mid- and end-diastole phases of the cardiac cycle.
(vi) The longitudinal movement (mm) of four points (S, L, A and P) on the TA, between end-systole and end-diastole phases of the cardiac cycle.
(vii) Tethering distance of the TV (determined as shown in Fig. 3).

Analysis of the tricuspid annulus flexibility

Prior to analysing the dynamic movement of the TA, we needed to develop a program to track the annulus, since the annulus does not have an outline, i.e. the boundary between the annulus and surrounding tissues is quite obscure. Our program, which was semiautomatic, was a modification of that developed by Oka and colleagues [15], which used 2D continuous dynamic programming and weak-spotting to accurately track annulus movement. First, six slices were obtained at 12 mm intervals, by parallel imaging in the four-chamber view. Twelve points bisecting the annulus were manually traced and an outline of the annulus was automatically created using a 3D spline-curving procedure [16]. Subsequently, the system automatically tracked the movement of the traced points through sequential parallel image slices and created a 3D animation from these MRI motion slices using Swing and Java

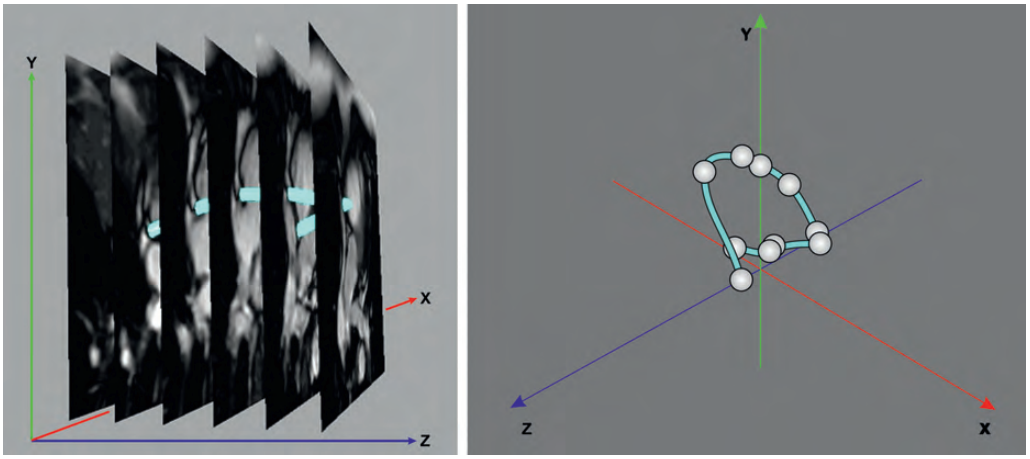

Figure 4: Tricuspid annulus (TA) point tracking and determination of TA orbital volume. The movement of points on the TA was tracked through six sequential, parallel MRI slices. 3D movement was determined by superimposing the images on an *x*, *y* and *z* planes (left). The orbital path, along the *y*-axis, was determined and the enclosed area (orbital area) was calculated (right).

Table 1: Basic and clinical characteristics and RVEF (%), RV-EsA and RV-EdA indices (mm^2/m^2) and RV-EdV index (ml/m^2)

	Healthy subjects (*n* = 20)	Patients with FTR (*n* = 19)	*P*-value
Age	32.2 ± 9.4	76.8 ± 7.0	<0.001
Gender (male/female)	10/10	11/8	0.863
Body weight (kg)	59.5 ± 12.9	50.2 ± 12.5	0.050
Diabetes mellitus	0	6	0.008
hyperlipaemia	1	5	0.091
Hypertension	0	14	<0.001
Previous stroke	0	0	1.000
Lung disease	0	4	0.047
Renal disease	0	2	0.231
Chronic atrial fibrillation	0	9	<0.001
Smoker	3	2	1.000
RVEF (%)	49.6 ± 5.3	39.8 ± 6.8	0.012
RV-EsA index (mm^2/m^2)	677.2 ± 113.9	731.1 ± 183.6	0.347
RV-EdA index (mm^2/m^2)	1280.5 ± 221.0	1325.2 ± 168.3	0.597
RV-EdV index (ml/m^2)	50.8 ± 9.4	55.8 ± 13.4	0.403

RVEF: right ventricular ejection fraction; RV-EsA: right ventricular end-systolic area; RV-EdA: right ventricular end-diastolic area; RV-EdV: right ventricular end-diastolic volume; FTR: functional tricuspid regurgitation.

3D software (Supplementary Video S1). In order to identify the 3D position of the tracked points, *x*, *y* and *z* coordinates were established and used for integrated TAA movement along the *y*-axis (the longitudinal vector) throughout the cardiac cycle. This allowed us to determine the orbiting volume of the annulus (Fig. 4).

Statistical analyses

All values are presented as mean ± SD. Comparison of quantitative parameters between the healthy subjects and in patients with FTR was made using unpaired *t*-tests for numerical data and χ^2 or Fisher's exact tests for categorical data. Two-way repeated-measures ANOVAs, followed by *post hoc* testing with the Bonferroni corrections were used to compare the AP and LS distances and the TAA between the study groups during phases (mid- and end-systole and mid- and end-diastole) of the cardiac cycle.

Differences were considered significant if $P < 0.001$. A SigmaPlot package (SigmaPlot, version 11, Systat Software INC, CA, USA) was used for statistical analyses. This software uses the Kolmogorov–Smirnov test to test for a normally distributed population.

RESULTS

Baseline demographic and clinical characteristics of healthy subjects and FTR patients are presented in Table 1. Patients with FTR were significantly older than healthy subjects and were slightly male-dominant, but body weight and height were similar between the two groups. Of the FTR patients, six had diabetes, five hyperlipemia, four lung disease, two chronic renal disease and nine chronic atrial fibrillation. Among the healthy subjects, one had hyperlipemia and three were smokers.

Among the patients, the mean left ventricular ejection fraction (%) was 54.6 ± 12.1, and left-ventricular end-systolic and end-diastolic dimensions (mm) were 36.1 ± 9.9 and 51.2 ± 9.1, respectively. Moderate tricuspid regurgitation was found in 16 patients, and severe tricuspid regurgitation in 3. The mean

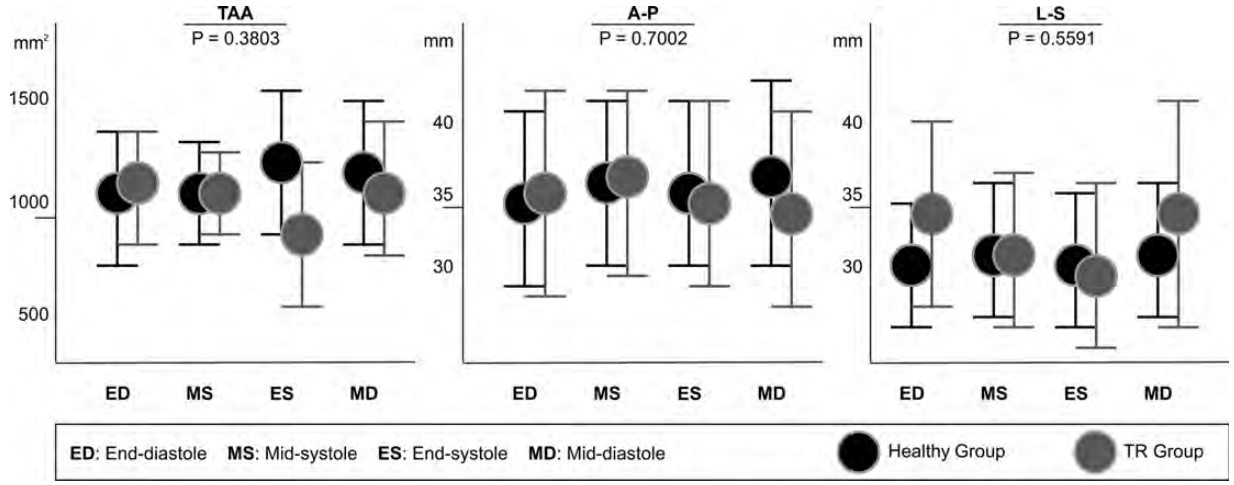

Figure 5: Comparison of the tricuspid annular area (mm^2), AP distance (mm) and LS distance (mm) during the cardiac cycle between in healthy subjects and in patients with functional tricuspid regurgitation.

Table 2: Comparison of the longitudinal moving distance (mm) of points S, L, A and P on the tricuspid annulus (TA) and the tethering height (mm) of tricuspid leaflets

	Point on the TA				Tethering height
	S	L	A	P	
Healthy subjects	12.7 ± 2.3	21.4 ± 3.7	16.3 ± 2.8	17.8 ± 3.3	4.0 ± 1.3
Patients with FTR	5.3 ± 2.9	12.3 ± 3.7	9.8 ± 3.2	10.0 ± 4.2	9.6 ± 1.5
P-value	<0.001	<0.001	<0.001	<0.001	<0.001

FTR: functional tricuspid regurgitation.

pressure gradient (mmHg) across the TV was 37.4 ± 9.1. RVEF (%) and RV-EsA and RV-EdA indices (mm^2/m^2) were 49.6 ± 5.3, 677.2 ± 113.9 and 1280.5 ± 221.0, respectively, in healthy subjects and 39.8 ± 6.8, 731.1 ± 183.6 and 1325.2 ± 168.3, respectively, in patients with FTR. The RV-EdV index (ml/m^2) was 50.8 ± 9.4 in healthy subjects and 55.8 ± 13.4 in patients with FTR. These values did not differ between the two groups (Table 1). The mean TAA (mm^2), AP distance (mm) and LS distance (mm), from mid- to end-systole and mid- to end-diastole phases, also did not differ between the two groups (Fig. 5). The 3D structure of the TA appeared normal in both groups; with anteroseptal points located at the farthest and posteroseptal points located closest to the apex. Despite the normal TA structure, the longitudinal moving distances (mm) of TA points differed between the two groups. The mean distances of S, L, A and P movement in healthy subjects (12.7 ± 2.3, 21.4 ± 3.7, 16.3 ± 2.8 and 17.8 ± 3.3, respectively) were significantly longer than those measured in FTR patients (5.3 ± 2.9, 12.3 ± 3.7, 9.8 ± 3.2 and 10.0 ± 4.2, respectively; Table 2). In addition, the tethering heights (mm) in healthy subjects were significantly smaller than in patients with FTR (4.0 ± 1.3 vs 9.6 ± 1.5, respectively; $P < 0.001$; Table 2). Animations of TA movement were created for each case to confirm differences in longitudinal flexibility between groups. The results of these animations confirmed the above findings. They indicated that the normal 3D structure of the TA was maintained in both groups during longitudinal movement, but the integrated orbiting volume (mm^3) of the TAA, as it moved throughout the cardiac

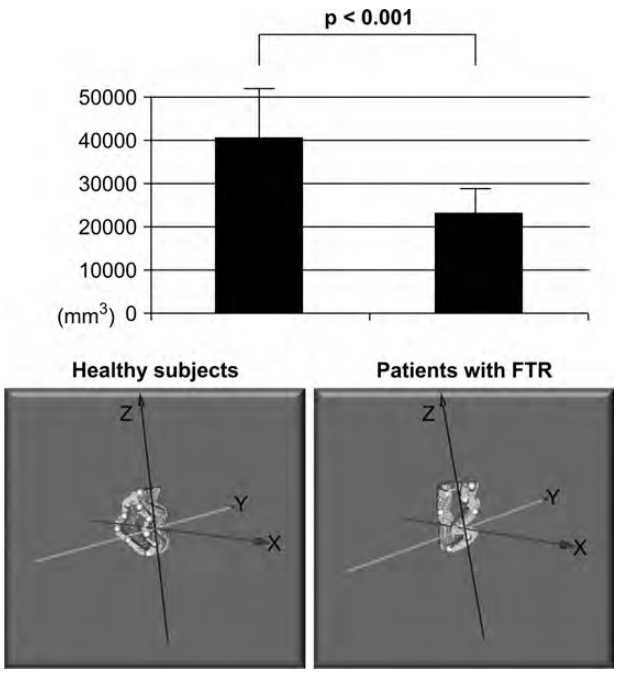

Figure 6: Comparison of the integrated orbiting volume of the tricuspid annulus. Integrated volume of the annular moving track throughout the cardiac cycle was significantly larger in healthy subjects than in patients with functional tricuspid regurgitation.

cycle, was significantly larger in healthy subjects than in patients with FTR (40428 ± 10951 vs 22967 ± 6079, respectively; $P < 0.001$; Fig. 6).

DISCUSSION

The dilation of the RV and resulting dilation and planarization of the TA and the tethering of the tricuspid leaflets are considered the primary cause of FTR in patients with myocardial dysfunction [1–3]. Previous geometric assessments of the TA, using real-time 3D echocardiography, have shown that the TA achieves a non-planar and non-circular shape during the systole phase [9, 10]. This geometric change seems as if it would contribute to correct coaptation of the three leaflets. However, the same geometry is observed in both healthy subjects and patients with FTR, indicating an alternative pathological mechanism of FTR. In addition, FTR is not always associated with the dilation of the RV and the flattening of the TA.

In this study, as a preliminary investigation for alternative mechanisms of FTR, we targeted patients with moderate or severe FTR and non-dilated RV to assess TA flexibility. Interestingly, we found that the 3D structure of the TA was maintained and the annulus was not significantly dilated in patients with FTR, yet the tethering distance was significantly longer than in healthy subjects. We hypothesize that the tethering distance was greater, despite the absence of RV and TA dilation, because of loss in the longitudinal flexibility of the TA.

The longitudinal moving distances, of all points on the TA, were significantly longer in healthy subjects than in patients with FTR. On the systolic phase, the TA of healthy subjects was flexible and moved vertically towards the apex to reduce the tethering height and allow the adequate coaptation of the tricuspid leaflets. In contrast, the TA in patients with FTR was less flexible and their longitudinal movement was more restricted. Accordingly, the distance between the TA plane and the ventricular apex during the systolic phase was greater, increasing the tethering distance of the tricuspid leaflets.

Several studies suggest that left ventricular ejection fraction is a poor indicator of early myocardial dysfunction, whereas the longitudinal myocardial velocity, strain and strain ratio appear to be more sensitive and specific identifiers of early ventricular dysfunction [17–19]. In addition, the movement of the TA plane during the systolic phase is known to be correlated with RV function [20, 21]. Therefore, it is possible that the onset of RV dysfunction can be initiated by the loss of longitudinal myocardial contractility prior to the decrease in RVEF or the dilation of the ventricle. This may cause the loss of TA longitudinal flexibility in patients with early FTR before they develop RV dilation. Further investigation of the relation between the loss of TA longitudinal flexibility and the tethering of tricuspid leaflets is necessary to unravel the initial mechanism of FTR.

The results of this study may indicate why annuloplasty is not 100% effective in eliminating FTR. While tricuspid annuloplasty involving the insertion of a prosthetic band is the preferred intervention [7, 8] for FTR, this procedure was designed to address the dilation and flattening of the TA. Theoretically, no band or ring used for tricuspid annuloplasty can improve the loss of the longitudinal TA flexibility, so that it should be difficult, even with a 3D rigid band, to perfectly eliminate FTR associated with the tethering of leaflets. Persistent residual tricuspid regurgitation after ring annuloplasty is correlated with the degree of the tethering [8]. It remains unclear if the vertical rearrangement of the TA by the 3D rigid band, in which the vertical geometric gap is only 2 or 3 mm, can truly reduce the tethering of leaflets. It is likely that we need to develop the new technique to reduce the residual tethering, particularly when patients have the seriously tethered valves associated with pulmonary hypertension (PH) or dilated RV. Some reports [12, 22] suggest that an additional procedure, such as the pericardial patch augmentation of the anterior leaflet, is recommended to terminate a severe tricuspid regurgitation associated with the tethering. Further investigation is necessary to confirm the benefits of such additional procedures or to determine if tricuspid replacement is necessary.

This study demonstrated that cardiac MRI can be used for the geometric assessment of TA flexibility. Geometric assessment by real-time 3D echocardiography can also provide clear images of the annular structure. However, deriving accurate and reliable quantitative data from these images is difficult because echovectors are variable, depending on the location of the ribs and lungs. Cardiac MRI, with its superior tissue contrast and high spatial and temporal resolution, enabled the accurate tracing of specific points on the TA. Using a new program that we developed, we were able to track the movement of these points during the cardiac cycle, quantify distances and TA orbital volume and assess TA flexibility. This system also creates dynamic animations (4D images), enabling the user to monitor changes that occur during the cardiac cycle. This system may not be limited to investigations of the TA and may be equally well suited for investigations of other heart structures (e.g. the mitral annulus or papillary muscles).

While the results of this study indicate the loss of TA longitudinal flexibility and demonstrate a novel system for 4D imaging, we recognize that it also has a few limitations. First, the study population was relatively small and restricts our ability to conclude whether our findings can be applied to a broader population of FTR patients. Second, the healthy subjects (our control group) were significantly younger than the patients with FTR; thus, age is a potential confounding factor in this study and may have contributed to the differences in annular flexibility that we observed between groups. Third, all healthy subjects had normal sinus rhythm, but nine patients with FTR showed chronic atrial fibrillation associated with left-sided heart disease. This could have affected the dynamic data (movement of the TA) in patients with FTR. Fourth, pulmonary hypertension in some cases was amalgamated in FTR patients, which could be one of the factors triggering the development of FTR in the absence of RV enlargement. It is certain that the patients with left-sided heart disease can have more developed pulmonary hypertension. However, the main mechanism of FTR is considered to be annular dilatation and the tethering of the leaflets subsequent to RV dilatation. Even severe pulmonary hypertension does not necessarily cause notable FTR. Hence, it currently remains unclear how PH directly damages the correct coaptation of tricuspid leaflets. Finally, since we did not assess RV function using pulse-wave Doppler tissue imaging, we are unable to describe the relationship between TA flexibility and RV long-axis dysfunction.

In conclusion, we analysed the 4D geometry of the TA in healthy subjects and in patients with FTR and non-dilated RV. The longitudinal flexibility of the TA in FTR was significantly less than in healthy subjects. This loss of longitudinal flexibility may cause the tethering of tricuspid leaflets, as suggested by the greater tethering height we observed in FTR patients. On the basis of these findings, a mechanism, by which early FTR can develop

independent of dilation and loss of TA curvature, should be elucidated to eliminate FTR. The system we have developed here, for the 4D geometric assessment of TA function using cardiac MRI, provides an excellent modality to assess the TA flexibility.

SUPPLEMENTARY MATERIAL

Supplementary material is available at *ICVTS* online.

ACKNOWLEDGEMENTS

We thank Ryuichi Oka and his colleagues at the Aizu University School of Computer Science and Engineering for the development of a new dynamic programming to track the TA and the creation of the TA dynamic four-dimensional animation.

Conflict of interest: none declared.

REFERENCES

[1] Mikami T, Kudo T, Sakurai N, Sakamoto S, Tanabe Y, Yasuda H. Mechanisms for development of functional tricuspid regurgitation determined by pulsed Doppler and two-dimensional echocardiography. Am J Cardiol 1984;53:160–3.
[2] Come PC, Riley MF. Tricuspid annular dilatation and failure of tricuspid leaflet coaptation in tricuspid regurgitation. Am J Cardiol 1985;55:599–601.
[3] Sagie A, Schwammenthal E, Padial LR, Vazquez de Prada JA, Weyman AE, Levine RA. Determinants of functional tricuspid regurgitation in incomplete tricuspid valve closure: Doppler color flow study of 109 patients. J Am Coll Cardiol 1994;24:446–53.
[4] Bernal JM, Gutierrez-Moriote J, Llorca J, San Jose JM, Morales D, Revuelta JM. Tricuspid valve repair: an old disease, a modern experience. Ann Thorac Surg 2004;78:2069–74.
[5] Frater R. Tricuspid insufficiency. J Thorac Cardiovasc Surg 2001;122:427–9.
[6] Nath J, Foster E, Heidenreich PA. Impact of tricuspid regurgitation on long-term survival. J Am Coll Cardiol 2004;43:405–9.
[7] McCarthy PM, Bhudia SK, Rajeswaran J, Hoercher KJ, Lytle BW, Cosgrove DM *et al*. Tricuspid valve repair: durability and risk factors for failure. J Thorac Cardiovasc Surg 2004;127:674–85.
[8] Fukuda S, Song JM, Gillinov AM. Tricuspid valve tethering predicts residual TR after tricuspid annuloplasty. Circulation 2005;111:975–9.
[9] Fukuda S, Saracino G, Matsumura Y, Daimon M, Tran H, Greenberg NL *et al*. Three-dimensional geometry of the tricuspid annulus in healthy subjects and in patients with functional tricuspid regurgitation: a real-time, 3-dimensional echocardiographic study. Circulation 2006;114(Suppl I):I-493–8.
[10] Ton-Nu TT, Levine RA, Handschumacher MD, Dorer DJ, Yosefy C, Fan D *et al*. Geometric determinants of functional tricuspid regurgitation: insight from 3-dimensional echocardiography. Circulation 2006;114:143–9.
[11] Jeong DS, Kim KH. Tricuspid annuloplasty using the MC3 ring for functional tricuspid regurgitation. Circ J 2010;74:278–83.
[12] Roshanali F, Saidi B, Mandegar MH, Yousefnia MA, Alaeddini F. Echocardiogeaphic approach to the decision-making process for tricuspid valve repair. J Thorac Cardiovasc Surg 2010;139:1483–7.
[13] Haddad F, Hunt SA, Rosenthal DN, Murphy DJ. Right ventricular function in cardiovascular disease, part I anatomy, physiology, aging, and functional assessment of the right ventricle. Circulation 2008;117:1436–48.
[14] Zornoff LA, Skali H, Pfeffer MA, St John Sutton M, Rouleau JL, Lamas GA *et al*. Right ventricular dysfunction and risk of heart failure and mortality after myocardial infarction. J Am Coll Cardiol 2002;39:1450–5.
[15] Oka R. General Scheme of Continuous Dynamic Programming Optimal Full Matching for Spotting Image. IEICE Technical Report, PRMU2010-87, IBISML2010-59 (2010-09).
[16] Ballard DH, Brown CM. Computer Vision. Englewood Cliffs, NJ: Prentice-Hall, 1982.
[17] Nahum J, Bensaid A, Dussault C, Macron L, Clemence D, Bouhemad B *et al*. Impact of longitudinal myocardial deformation on the progress of chronic heart failure patients. Circ Cardiovasc Imaging 2010;3:249–56.
[18] Richand V, Lafitte S, Reant P, Serri K, Lafitte M, Brette S *et al*. An ultrasound speckle tracking (two-dimensional strain) analysis of myocardial deformation in professional soccer players compared with healthy subjects and hypertrophic cardiomyopathy. Am J Cardiol 2007;100:128–32.
[19] Koyama J, Ray-Sequin PA, Falk RH. Longitudinal myocardial function assessed by tissue velocity, strain, and strain rate tissue Doppler echocardiography in patients with AL (primary) cardiac amyloidosis. Circulation 2003;107:2446–52.
[20] Lopez-Candales A, Rajagopalan N, Saxena N, Gulyasy B, Edelman K, Bazaz R *et al*. Right ventricular systolic function is not the sole determinant of tricuspid annular motion. Am J Cardiol 2006;98:973–7.
[21] Miller D, Farah MG, Liner A, Fox K, Schluchter M, Hoit BD. The relation between quantitative right ventricular ejection fraction and indices of tricuspid annular motion and myocardial performance. J Am Soc Echocardiogr 2004;17:443–7.
[22] Dreyfus GD, Raja SG, Chan KMJ. Tricuspid leaflet augmentation to address severe tethering in functional tricuspid regurgitation. Eur J Cardiothorac Surg 2008;34:908–10.